# MCNPX-PoliMi simulation capacity using thermal neutron cross-sections to assess the reliability of the neutron multiplicity mass analysis where shielding is unknown

**Malte Göttsche[1] and Gerald Kirchner[1]**

**Abstract:** In the context of warhead authentication in a future arms control verification regime, neutron multiplicity measurements are useful to determine plutonium mass which may be used as a warhead indicator. The inspecting party might have little knowledge on possible shielding between plutonium component and detector, as this may be sensitive information which however has an influence on the mass output of the multiplicity analysis. To investigate the confidence an inspector can have from neutron multiplicity measurements of unknown configurations, a systematic analysis of its possibilities and limitations must be performed. MCNPX-PoliMi simulations are helpful in this regard. As a first step the code's functionality was investigated comparing simulation results to experimental data of plutonium neutron multiplicity measurements using a He-3 detector. Thermal neutron cross-sections for the moderating material in the detector are required for a successful simulation, as scattering with the lattice structure becomes relevant. Scattering can be described by the creation and annihilation of phonons, the cross-sections are obtained from the phonon excitation spectrum. Taking into account statistical and systematic simulation uncertainties, the deviation to the measurement data generally lies within the simulation uncertainty.

## Introduction

In most situations where radioactive samples are characterized, certain knowledge exists prior to the measurements. The geometry and other properties might be known, at least roughly. Quantitative analysis methods can rely on detector calibration with representative standards of known density and geometry. In warhead authentication as part of a future arms control verification regime, this is not the case; warhead or warhead component design information will not be available, there may also be additional unknown shielding. This raises the problem that a designed system must authenticate an item whose configuration such as geometry remains largely unknown. Therefore the optimum measurement system should be chosen in such a way that it does not depend on calibration with materials representative of the warhead or component and that a minimum number of assumptions has to be made regarding the nature of the item.

We investigate one potential measurement technique – neutron multiplicity counting – in regard to its advantages and limitations for plutonium warhead authentication. Therefore we assess different item and shielding configurations to see to which extent and why measurement results (plutonium mass) differ from the actual values. Only a very limited choice of sample configurations is available for measurements, so that Monte Carlo simulations must be the main tool for such an analysis. As the first step, we have conducted measurements in order to test

whether the simulation code functions properly in regard to our purposes. The results of this study are covered in this paper.

## Neutron multiplicity counting

As a warhead requires a certain plutonium mass in order to work, assessing an item's plutonium mass (with an information barrier) can be considered an indicator that it is a warhead. In order to deduce the plutonium mass through passive neutron counting, the spontaneous fission rate would need to be measured from which the $^{240}Pu$ mass could be deduced. Then, the total plutonium mass can be calculated when the isotopic composition is known, e.g. by gamma spectroscopy.

The neutron flux emitted by a fissile sample is affected by a number of possibly unknown properties:

• Total spontaneous fission rate which depends on the fissile mass

• Neutron multiplication across the sample, in particular from induced fission by Pu-239

• $(\alpha, n)$ reactions if oxides are present

This process can be described by the "superfission model": One or several initial neutrons are emitted by a spontaneous fission or $(\alpha, n)$ reaction, which can then induce fission (and the process continues with the neutrons produced by the induced fission). The sum of all these neutrons is then the result of a "superfission" process (assuming that all neutrons from one process are emitted simultaneously) which includes the three described events. The number of neutrons emitted by this process follows a probability distribution, called the emitted multiplicity distribution which is a combination of the multiplicity distributions for $^{240}Pu$ spontaneous fission and $^{239}Pu$ induced fission as well as the uncorrelated $(\alpha, n)$ reactions. It can be described analytically as a function of the three unknown neutron sources.[2,3]

Passive neutron multiplicity counting is a technique that opens a gate when a neutron is detected which collects the coincident neutrons while it is open. This measured multiplicity distribution can be related to the emitted multiplicity distribution. Specifically, the first three moments of the distribution called the Singles (S), Doubles (D) and Triples (T) rates are used to calculate the first three moments of the emitted distribution. From measuring S, D and T, one can solve for the three unknowns, so that the fissile mass can be calculated from the spontaneous fission rate and the isotopic composition.

Typically, He-3 detectors are used for multiplicity analyses. Since the He-3 neutron capture cross-section decreases with the energy, fast neutrons are thermalized by polyethylene surrounding the He-3 tubes. The mean neutron lifetime (die-away time) is in the range of tens of microseconds (depending on the detector), so that coincidence gates must remain open for a sufficient time (usually $32 - 64\ \mu s$). For such gate lengths, also uncorrelated background events will be detected besides the correlated events. This requires also randomly triggered gates with only uncorrelated events to subtract those from the events in the coincidence gate to obtain the real coincidences. Furthermore, there will be correlated neutrons that enter the detector after the

coincidence gate is closed. The ratio of the correlated events counted in the gate to the total number of correlated events is called gate fraction, which is also needed to calculate the emitted multiplicity moments.

## Measurements and simulations

In order to check the Monte Carlo code`s neutron multiplicity simulation capacities, we have conducted neutron multiplicity measurements of plutonium samples. The measurements were done at the Institute for Transuranium Elements of the Joint Research Centre in Ispra, Italy, at the PERLA laboratory.

The available samples were three metal samples (12-19 g, $^{240}Pu$ content 4-9%), four 6.7 g oxide samples with different isotopic compositions ($^{240}Pu$ content 6-25%), four oxide samples with the same isotopic composition ($^{240}Pu$ content 13.2%) and different masses (2-20 g) and combinations thereof. Information on three of the samples is given in Table 1. In addition, data from a $^{252}Cf$ measurement was used (5227 neutrons/second yield).[4]

The available detector was the Passive Scrap Multiplicity Counter (PSMC) which is a high efficiency neutron counter that is well-suited for multiplicity analyses of smaller samples. Its efficiency is >54% for $^{240}Pu$ spontaneous fission neutrons. The sample cavity has a size of 20x40 cm.[5] A sketch of the detector can be seen in Figure 1. The He-3 tubes are surrounded by a high-density polyethylene moderator. The assay cavity is lined with a 1 mm cadmium liner. The active length of the He-3 tubes is 711 mm; their outer diameter is 25.4 mm. The detector has a gate width setting of 64 $\mu s$.[6]

The simulation codes that are compared to the experimental data are MCNPX[7] and MCNPX-PoliMi[8] which have neutron multiplicity simulation capacities. Similar tests had been performed in the past, in particular the ESARDA Multiplicity Benchmark Exercise.[9] Therefore one purpose of our exercise was to extend the tests to the PSMC which was not included earlier, to perform a more detailed analysis of the uncertainties and to check whether deviations of MCNPX/MCNPX-PoliMi simulations from the measurements are within these uncertainties.

Both MCNPX and MCNPX-PoliMi derive the S, D and T rates. MCNPX directly analyses the real coincidences without simulating the real experimental setup with the uncorrelated neutrons, while MCNPX-PoliMi fully simulates the coincidence gate and the randomly triggered gate, so that the uncorrelated events can be subtracted from the neutrons of the coincidence gate to obtain the real coincidences.

## Thermal neutron scattering

With standard nuclear MCNP cross-sections, one obtains large deviations between multiplicity measurements and simulations. The D and T rates are systematically overestimated by 6-17% and 10-35%, which would make multiplicity simulations essentially useless. Such deviations cannot be explained by systematic uncertainties of the detector geometry or nuclear data.

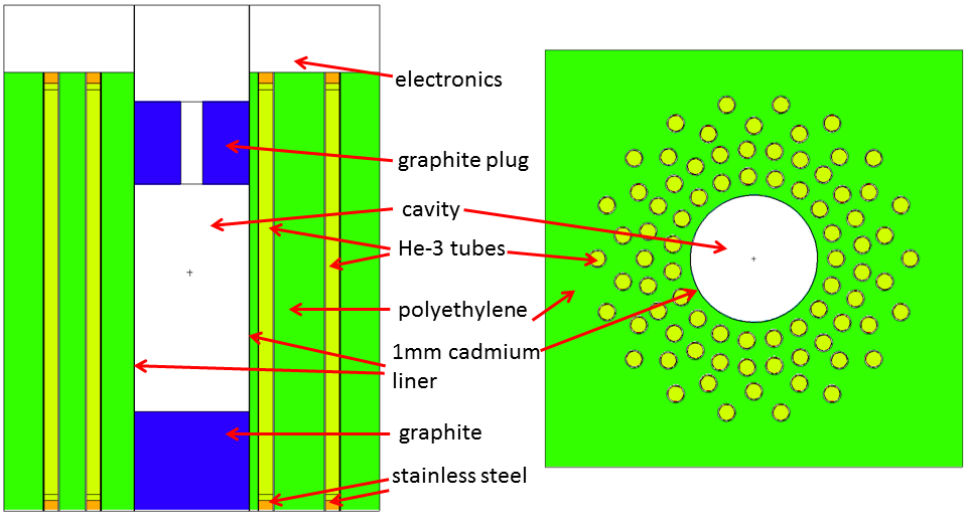


Figure 1: Model of the Passive Scrap Multiplicity Counter. White indicates air or materials of little relevance for neutron transport, blue indicates graphite, orange indicates stainless steel, the shiny green indicates polyethylene, the greenish yellow indicates He-3. The total size of the detector is 661 x 661 x 942 mm (length x width x height).

| | type | Pu mass [g] | $^{238}Pu$ [wt-%] | $^{239}Pu$ [wt-%] | $^{240}Pu$ [wt-%] | $^{241}Pu$ [wt-%] | $^{242}Pu$ [wt-%] | $^{241}Am$ [wt-%] |
|---|---|---|---|---|---|---|---|---|
| PM1 | metal | 12.5 | 0.00 | 95.42 | 4.53 | 0.03 | 0.02 | 0.25 |
| $PuO_2$ 10 | oxide | 2.0 | 0.06 | 86.08 | 13.27 | 0.32 | 0.27 | 1.48 |
| CBNM 61 | oxide | 5.8 | 1.03 | 65.84 | 26.70 | 2.02 | 4.42 | 6.36 |

Table 1: Characteristics of measured samples

The reason is that for thermal neutrons, the de Broglie wavelength becomes sufficiently large that they interact also with the chemical bonding structure, in our case polyethylene. A general quantum-mechanical scattering kernel describing the thermal neutron cross-sections can be derived.[10,11,12] Cross-sections are obtained by applying Fermi's Golden Rule (which describes the transition rate from one initial energy eigenstate of a quantum system to eigenstates after a perturbation by a potential) and the definition of the scattering amplitude $f(\vec{k},\overrightarrow{k'})$ which is a function of the appropriate wave function of the system and the potential of the scatterer:[13]

$$\frac{d\sigma}{d\Omega} = \frac{k'}{k}\left|f(\vec{k},\overrightarrow{k'})\right|^2$$

where $\vec{k}$ is the wave vector of the initial and $\overrightarrow{k'}$ is the wave vector of the final state. The result is[14]

$$\sigma(E \to E', \mu) = \frac{c}{2kT}\sqrt{\frac{E'}{E}}S(\alpha,\beta)$$

where $E$ and $E'$ are the incident and final neutron energies, $\mu$ is the cosine of the scattering angle, $c$ is a material-specific constant, $kT$ is the thermal energy and $S(\alpha, \beta)$ is the so-called scattering law which depends on the momentum transfer $\alpha$ and the energy transfer $\beta$.

The scattering law must be evaluated for the specific scatterer. For crystalline solids, it can be assumed that the individual atoms in a lattice act as coupled harmonic oscillators, where the vibrations are described by phonons.[15] There is elastic and inelastic scattering. In this case (and in contrast to elastic scattering on free atoms), elastic scattering does not include kinetic energy transfer between the neutron and the scatterer, since the scatterer's mass (considering the entire lattice) is much larger than the neutron's. Inelastic scattering results in an energy loss or gain of the neutrons. Since the scatterer is in thermal motion, it can actually transfer energy to a thermal neutron. The neutron can transfer energy to the scatterer and thereby excite it which corresponds to the production of phonons in a crystalline material.[16] A single neutron may create a couple of phonons, or no phonons at all. The latter is the case of elastic scattering. The scattering law can be expressed by the material-specific frequency spectrum of excitations (phonons) in the system $\rho(\beta)$.

Polyethylene consists of long hydrocarbon chains and is partially crystalline. To arrive at a theoretical frequency spectrum, the chains can be assumed to be infinitely long. The long molecules are in a zig-zag shape with the $CH_2$ radicals at each vertex. The coupling between neighboring chains is rather weak so that the spectrum can be derived from evaluating a single chain.[17] In polyethylene, vibrations include stretching, bending, wagging, rocking, torsion and twisting. Nine major modes comprised of these types have been identified. From the frequency spectrum, the scattering cross-sections can be calculated using the equations given above.

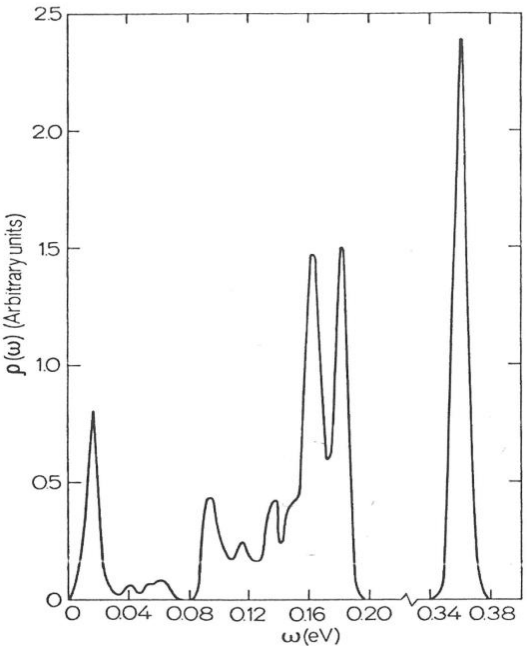


Figure 2: Frequency spectrum for the polyethylene chain used in the neutron calculations, taken from *D. Sprevak and J.U. Koppel, Neutron Scattering by Polyethylene, Nukleonik 12, 1969*

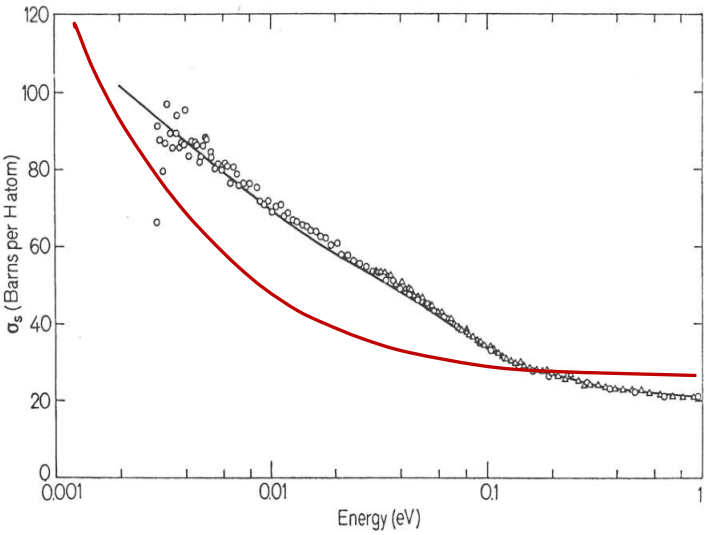


Figure 3: The derived (black line) and measured (dots) total thermal polyethylene cross-section is shown, taken from *D. Sprevak and J.U. Koppel, Neutron Scattering by Polyethylene, Nukleonik 12, 1969*.
The red line represents the total nuclear cross-section.

Sprevak and Koppel[18] have performed these two steps, their results can be seen in Figure 2 and Figure 3. The agreement between theory and experiment is excellent.

These thermal cross-sections can be called by MCNP upon user input. A grid of $S(\alpha, \beta)$ for all different values for $\alpha$ and $\beta$ has been calculated, which enables the appropriate thermal cross-sections to be sampled accordingly. If this option is chosen, MCNP overrides the nuclear cross-sections with the thermal cross-sections below 4 eV, although the effects are most significant below 2 eV.[19]

## Uncertainties

The detector geometry implemented in MCNPX/MCNPX-PoliMi is based on available sketches from the detector manufacturer.[20] Unfortunately, the resolution of the sketch is low and no further information could be obtained. Therefore, the MCNP code check was used to optimize the implemented detector design through searching for the simulation results that best resembled the measurement results. A variety of parameters was identified whose values were not exactly known. These were changed in plausible ways so that all investigated values were consistent with the available information. This way, the optimal parameter values were identified; furthermore a sensitivity analysis was obtained for the individual parameters from which the uncertainties of the finally implemented detector model can be estimated.

The types of uncertainties and their variations are listed in Table 2, including detector and sample geometry as well as nuclear data uncertainties. Their influence on the Singles, Doubles and Triples rates is listed in Table 3, which also compares the measurements and the simulation results using the optimized detector design for four different samples.

| Type | Influence | Estimate |
|---|---|---|
| Vertical position of He-3 tubes | Influence on $\epsilon$ as neutron flux from a source placed in the middle of the detector is different at various tube heights - being maximal at the same height as the source. A very similar effect is due to an uncertainty in the active length of the He-3 tubes.[21] | $\pm 1\ cm$ |
| horizontal position of He-3 tubes | Influence on $\epsilon$ and gate fraction. The closer the He-3 tubes are to the cavity, the smaller is the die-away time as neutrons travel through less polyethylene before being detected, thus increasing the gate fraction. Through the change in moderation, $\epsilon$ is affected. With little moderation, neutrons are not slowed down ideally to be detected, with too much moderation, neutron capture in hydrogen outweighs the effect of better moderation. | $\pm 4\ mm$ |
| polyethylene density | Influence on $\epsilon$ and the gate fraction due to neutron moderation and capture and the influence on the die-away time. | $\pm 0.5\%$[22] |
| pressure of the He-3 gas | Direct influence on $\epsilon$ | $\pm 1\%$[23] |

| | | |
|---|---|---|
| cadmium liner thickness | It prevents neutrons that escaped the cavity to be reflected back, due to its high absorption cross-section for thermal neutrons. Our simulations show that detection rates are increased significantly only after reducing the thickness by a factor 10. | none |
| position of the sample within the cavity | The detection efficiency of the detector depends very little on the sample position, the position was measured well.[24] | none |
| uncertainties from the shift register electronics | The gate lengths were slightly changed in the simulation, but in all cases the results were much worse than for a gate length of $64\ \mu s$, so that it was assumed that the simulated gate lengths were exact. | none |
| dead-time | The dead-time effects at the count rates of the measured sources were assessed to be negligible. For higher count rates, corrections are required. | none |
| Sample mass and isotopic composition | These uncertainties mainly influence the spontaneous fission rate and the multiplication. | See Table 3 |
| multiplicity distribution moments of $^{240}Pu$ spontaneous and $^{239}Pu$ induced fission | The standard deviation is taken from the measurement data of different experiments, noting that the individual publications only list statistical uncertainties, while the standard deviation of the different measurement data is much larger.[25] The standard deviations of the $^{239}Pu$ moments are similar to those of $^{240}Pu$. | See Table 3 |
| plutonium fission and $(\alpha, n)$ rates | Data from known assessments are available[26] allowing the calculation of the standard deviations of the $^{240}Pu$ fission and plutonium oxide $(\alpha, n)$ rates, the uncertainty on the californium fission rate is given by Peerani.[27] | See Table 3 |
| Sample safety containers | Reasonable variations in the container designs were simulated with negligible effects. | none |
| statistical uncertainty | The measured statistical uncertainty is the standard deviation of the mean of multiple runs of measuring the same sample, the statistical uncertainty from the simulations is obtained applying a semi-empirical approach.[28] | See Table 3 |

Table 2: Description and estimation of systematic and statistical uncertainties

## Simulation results

In general, both MCNPX and MCNPX-PoliMi yield results which are in agreement with each other, taking the statistical uncertainties into account.

Only a representative range of measurement results is presented in Table 3. A total of 12 different plutonium metal and oxide sources have been measured. Calculating the mean deviation between simulation and measurement from all samples and taking the standard deviations of this mean, one obtains

$$\Delta S = -2.3\% \pm 3.2\%$$

$$\Delta D = 2.9\% \pm 3.5\%$$

$$\Delta T = 5.4 \pm 9.4\%$$

Although the identified uncertainties of the individual samples vary somewhat as can be seen from Table 3, they are similar and the standard deviations of $\Delta S, \Delta D$ and $\Delta T$ appear to be in agreement with the uncertainties addressed in Tables 2 and 3. It is refrained from performing an exact error propagation as various correlations of errors are difficult to quantify. Moreover, the uncertainty from the horizontal tube position alone suffices for explaining the overall uncertainty.

As the standard deviations of $\Delta S, \Delta D$ and $\Delta T$ are larger than $\Delta S, \Delta D$ and $\Delta T$ themself, the conclusion is that the relevant uncertainties have been identified, i.e. that there is no relevant systematic bias. No corrections to our implemented simulation model are required as the simulated results with their uncertainties are in agreement with the experimental results.

## Acknowledgements

We would like to thank the German Foundation for Peace Research for providing generous funding of this research project. We are very thankful to Dr. Paolo Peerani for his strong support of the overall project, in particular by enabling the measurement campaign at the PERLA laboratory, which was essential for our study.

| | | **meas. result [1/s]** | $\sigma_{stat}$ [%] | **Simul. result [1/s]** | $\sigma_{stat}$ [%] [29] | vert. tube pos. [%] | horiz. tube pos. [%] | poly-ethylene density [%] | gas pressure [%] | moments [%] | emission rates [%] | mass [%] | isotopic comp. [%] | **deviation [%]** |
|---|---|---|---|---|---|---|---|---|---|---|---|---|---|---|
| $^{252}$Cf | **S** | **2884.0** | 0.1 | **2835.4** | 0.1 | 0.5 | 2.0 | 0.2 | 0.2 | 0.2 | | | | **-1.7** |
| | **D** | **1547.0** | 0.2 | **1606.5** | 0.2 | 1.0 | 4.5 | 0.3 | 0.5 | 0.2 | $^{252}$Cf: 0.3 | n.a. | n.a. | **3.8** |
| | **T** | **470.0** | 0.5 | **519.2** | 0.5 | 1.5 | 7.5 | 0.5 | 1.5 | 0.9 | | | | **10.5** |
| PM1 | **S** | **360.2** | 0.5 | **342.2** | 0.1 | 0.5 | 2.0 | 0.2 | 0.2 | 0.2 | | | | **-5.0** |
| | **D** | **137.9** | 0.5 | **136.5** | 0.2 | 1.0 | 4.5 | 0.3 | 0.5 | 0.8 | $^{240}Pu$: 1.1 | 2.4 | $^{239}Pu$: 0.0 $^{240}Pu$: 0.7 | **-1.0** |
| | **T** | **42.2** | 1.1 | **41.5** | 0.5 | 1.5 | 7.5 | 0.5 | 1.5 | 2.5 | | | | **-1.8** |
| $PuO_2$ 10 | **S** | **250.6** | 0.1 | **258.0** | 0.1 | 0.5 | 2.0 | 0.2 | 0.2 | 0.2 | | | | **2.9** |
| | **D** | **50.6** | 0.7 | **51.9** | 0.3 | 1.0 | 4.5 | 0.3 | 0.5 | 0.8 | $^{240}Pu$: 1.1 $(\alpha, n)$: 2.9 | n.a | n.a. | **2.4** |
| | **T** | **10.2** | 1.7 | **10.2** | 0.8 | 1.5 | 7.5 | 0.5 | 1.5 | 2.5 | | | | **-0.4** |
| CBNM 61 | **S** | **2287.5** | 0.2 | **2216.1** | 0.1 | 0.5 | 2.0 | 0.2 | 0.2 | 0.2 | | | | **-3.1** |
| | **D** | **393.6** | 0.2 | **406.6** | 0.4 | 1.0 | 4.5 | 0.3 | 0.5 | 0.8 | $^{240}Pu$: 1.1 $(\alpha, n)$: 2.9 | 0.8 | $^{239}Pu$: 0.0 $^{240}Pu$: 0.1 | **3.3** |
| | **T** | **84.0** | 0.5 | **93.2** | 1.0 | 1.5 | 7.5 | 0.5 | 1.5 | 2.5 | | | | **11.0** |

Table 3: Comparison of measured Singles, Doubles and Triples rates to the corresponding simulated values for four different samples including the deviation between simulation and measurement. For the experimental values, the statistical uncertainty is given, for the simulated values, the statistical uncertainties are given as well as further uncertainties addressed in the text. N.a. indicates that data were either not available or that the field is not applicable.

[1] Carl Friedrich von Weizsäcker-Centre for Science and Peace Research (ZNF), University of Hamburg, Beim Schlump 83, 20144 Hamburg, Germany, malte.goettsche@physik.uni-hamburg.de

[2] K.D. Böhnel, "The Effect of Multiplication on the Quantative Determination of Spontaneously Fissioning Isotopes by Neutron Correlation Analysis," *Nuclear Science and Engineering* 90 (1985): 75-82

[3] W.Hage and D. M. Cifarelli, "Correlation Analysis with Neutron Count Distributions in Randomly or Signal Triggered Time Intervals for Assay of Special Fissile Materials," *Nuclear Science and Engineering* 89 (1985): 159-176

[4] P. Federov, P. Peerani, B. Pedersen and M.M. Ferrer, "Calibration Procedures for the Plutonium Scrap Multiplicity Counter," Ispra (2005)

[5] Canberra, "PSMC-01- Plutonium Scrap Multiplicity Counter," C40093 (2013)

[6] "Calibration Procedures"

[7] D.B. Pelowitz, "MCNPX User's Manual Version 2.7.0," LA-CP-11-00438, Los Alamos (2011)

[8] S.A. Pozzi, S.D. Clarke, W.J. Walsh, E.C. Miller, J.L. Dolan, M.Flaska, B.M. Wieger, A. Enqvist, E. Padovani, J.K. Mattingly, D.L. Chicheser and P. Peerani, "MCNPX-PoliMi for Nuclear Nonproliferation Applications," *Nuclear Instruments and Methods in Physics Research Section A* 694 (2012): 119-125

[9] P. Peerani, M. Swinhoe, A-L. Weber and L.G. Evans, "ESARDA Multiplicity Benchmark Exercise – Phases III and IV," *ESARDA Bulletin* 42 (2009)

[10] M.M.R. Williams, *The Slowing Down and Thermalization of Neutrons* (Amsterdam: North-Holland Publishing Company, 1966)

[11] D.E. Parks, M.S. Nelkin, J.R. Beyster and N.F. Wikner, *Slow Neutron Scattering and Thermalization* (New York: W.A. Benjamin Inc, 1970)

[12] W. Marshall and S.W. Lovesey, *Theory of Thermal Neutron Scattering* (Oxford: Clarendon Press, 1971)

[13] "Theory of Thermal Neutron Scattering,", page 6

[14] "The Slowing Down and Thermalization of Neutrons"

[15] "The Slowing Down and Thermalization of Neutrons"

[16] R.E. MacFarlane, "Neutron Slowing Down and Thermalization," in *Handbook of Nuclear Engineering*, ed. D.G. Cacuci (New York: Springer Science+Business Media, 2010)

[17] D. Sprevak and J.U. Koppel, "Neutron Scattering by Polyethylene," *Nukleonik* 12 (1969)

[18] "Neutron Scattering by Polyethylene"

[19] X-5 Monte Carlo Team, "MCNP – A General Monte Carlo N-Particle Transport Code, Version 5," LA-CP-03-0245, Los Alamos (2003)

[20] "Canberra, PSMC-01"

[21] P. Peerani and A-L. Weber, "Analysis of Uncertainties Affecting the Monte Carlo Simulation of a Neutron Multiplicity Counter," *Radiation Measurements* 47 (2012): 475-480

[22] "Analysis of Uncertainties"

[23] "Analysis of Uncertainties"

[24] "Calibration Procedures"

[25] M. Zucker and N. Holden, "Parameters of Several Plutonium Nuclides and Cf-252 of Safeguards Interest," 6th ESARDA Conference, Venice (1984)

[26] P.M.J. Chard, S. Croft, M. Looman, P. Peerani, H. Tagziria, M. Bruggeman and A. Laure-Weber, "A Good Practice Guide for the Use of Modelling Codes in Non Destructive Assay of Nuclear Materials," *ESARDA Bulletin* 42 (2009)

[27] "Analysis of Uncertainties"

[28] S. Croft, M.T. Swinhoe and V. Henzl, "A Priori Precision Estimation for Neutron Triples Counting," 2nd International Conference on Advancements in Nuclear Instrumentation Measurement Methods and their Applications, Ghent (2011)

[29] The statistical uncertainty of the simulation is not in agreement with the measurement uncertainty as the simulations do not correspond to the same measurement times.